Batteries & Supercaps

Minireviews
doi.org/10.1002/batt.202000292

Chemistry Europe
European Chemical Societies Publishing

VIP *Very Important Paper*

Special Collection

A Minireview on High-Performance Anodes for Lithium-Ion Capacitors

Junsheng Zheng,*[a] Guangguang Xing,[a] Luyao Zhang,[a] Yanyan Lu,[a] Liming Jin,[a] and Jim P. Zheng[b]

Lithium-ion capacitors (LICs) are assembled with a battery-type anode and a capacitor-type cathode, so they combine high energy density of lithium-ion batteries (LIBs) and excellent rate and cycling performance of supercapacitors (SCs). However, the current level still cannot satisfy the target. And the leading problem is LICs cannot offer enough capacity under high power density and long cycling life due to the storage mechanism of anodes. This paper gives the present attempts on electrodes, solid–electrolyte interface (SEI) and operation conditions. And after discussion, the paper holds that the discharge voltage plateau of anodes should be well-chosen, and the anode structure like an ordered mesoporous structure can provide fast and versatile transport pathways for charge transfer and provide free space to accommodate the volume change upon Li-ions insertion/extraction. In addition, the multilayer SEI with the synergism like LiF and Li_2CO_3 can provide better electronic insulation and ion conductivity. Furthermore, appropriate working potential is also an effective mean to improve performance of LICs.

1. Introduction

Supercapacitors (SCs) are one of the commercial energy storage systems (ESSs) and their energy storage mechanism is the non-Faraday process, which offers it a high power density (1–10^3 $kW \cdot kg^{-1}$) and an excellent cycling stability (more than 10^6 times). However, it performs only a twentieth of the energy density of the batteries, such as LIBs, and that has become a challenge for its application. Nowadays the application developments require ESSs to show both high energy density and high power density, while LIBs perform poor power density and SCs exhibit poor energy density. Therefore, ESSs has attracted more and more attention in the industry due to its excellent energy density and power density.

A possible device is lithium-ion capacitors (LICs) which are composed of a capacitor-type cathode and a battery-type anode and combine the respective merits of LIBs and SCs. As shown in Figure 1a–b, the energy storage mechanism of LICs is Li-ions in the electrolyte insert into the negative electrode and the anions adsorb on the positive electrode during the charge process while ions undergo opposite migration during the discharge process. The first LIC was assembled with $Li_4Ti_5O_{12}$ as anode and activated carbon (AC) as cathode in 2001.[1] After that, different anodes and cathodes have been used as a potential component of LICs, such as AC//nitrogen-doped carbon,[2] multiwalled carbon nanotubes//TiO_2-B nanotubes,[3] and AC//expanded graphite.[4] The current LICs can achieve a maximum energy density of 20 $Wh \cdot kg^{-1}$ while the rate and cycling performances approach the level of SCs.

Together, LICs have three main advantages, including:

1) Compared with SCs, it has higher capacity and energy density, due to the improvement of anode materials capacity and the enlargement of working voltage range.
2) Compared with LIBs, it has higher power density, because of the rapid adsorption/desorption reactions on the positive electrode.
3) As a result of the limited damage on electrodes, LICs show better stability.

Although LICs are promising devices to meet requirements of some advanced ESSs, there is still a gap between the actual and desired values. For example, the United States Advanced Battery Consortium (USABC) requires the cell energy density of 30 $Wh \cdot kg^{-1}$ at 1 $kW \cdot kg^{-1}$ for start-stop battery.[5] And some insights about improving the cell energy density are given in Figure 1. The peaks in Figure 1c–d are close to 30 $Wh \cdot kg^{-1}$, it indicates that solely increasing one electrode capacity cannot increase the cell energy density indefinitely. And the curves in Figure 1e–f gradually tend to flat, it means that blindly pursuing high specific capacity of electrodes cannot improve the cell energy density. This is because asymmetric capacitors will consume ions in the electrolyte during the charging process, and the minimum mass of electrolyte required by the capacitor is even greater than the weight of the two electrodes.[6] And it is well accepted nowadays that using the pre-lithiated anode is helpful to improve the energy density of

[a] Dr. J. Zheng, G. Xing, L. Zhang, Y. Lu, L. Jin
Clean Energy Automotive Engineering Center and School of Automotive Studies
Tongji University
Shanghai 201804, China
E-mail: jszheng@tongji.edu.cn
[b] Prof. J. P. Zheng
Department of Electrical Engineering, University at Buffalo
The State University of New York
Buffalo, NY 14260, USA
E-mail: jzheng@buffalo.edu

Special Collection An invited contribution to a Special Collection dedicated to Metal-Ion – Hybrid Supercapacitors

LICs, and the improved capacity is given in region III and IV in Figure 1b. In addition, the gap between low kinetics of the intercalation electrodes and fast kinetics of the adsorption electrodes would lead to a mismatched region. It means that the energy density is sharply decreased when the power density is high. Improving the anodes kinetics to balance the difference is another mainstream problem of LICs.

When the electrode contacts with the electrolyte, there is a thermodynamic potential gap between them. As the cell voltage changes, electrochemical reactions between the electrode and the electrolyte is triggered, and new substances are generated at the interface of the two phases.[7] In 1979, E. Peled first found this interface on Li metal anode. This interface is called as solid–electrolyte interface (SEI) and it plays critical roles in balancing the cell potential. Due to the same storage mechanism of anodes between LIBs and LICs, there also is SEI in LICs. And the formation of SEI consumes electrolytes and Li-ions and it leads to loss capacity irreversibly.[11] And its insulation avoids the storage substances to be further consumed. However, attributed to the volume change of active particles, SEI will crack and regenerate continuously, and SEI will become thicker and thicker.[12] The continuous growth of SEI is one of the main factors for the capacity loss of modern Li-ion system.

From the above, to ameliorate anodes is the exerting points to obtain a better performance of LICs. In this paper, some outstanding achievements on improvement of anodes have been introduced during the past few years, in relation to the choice of materials, the design of electrodes, the modification of SEI and some operating strategies. Future perspectives for further development toward anodes in LICs are also proposed.

2. Achievements on Anode of High Performance LICs

As depicted in Figure 2a, introducing the battery-type anode into SCs is to increase the energy density, namely LICs. And from the storage mechanisms, it can be known that there is an

Dr. Junsheng Zheng is an Associate Professor at Tongji University. He obtained his Ph.D degree from East China University of Science and Technology in 2008. His research interests include advanced materials and novel structures for Lithium ion capacitor and fuel cell. He has published over 30 peer reviewed journal papers and possesses over 10 authorized patents in the field of fuel cells and Li-ion capacitor.

Liming Jin is a Ph.D candidate at the School of Automotive Studies of Tongji University. He obtained his B.S. degree at the Department of Chemical and Biological Engineering from Zhejiang University in 2016. His research interests include lithium ion batteries, lithium sulfur batteries and lithium ion capacitors.

Guangguang Xing is a graduate student at the School of Automotive Studies of Tongji University. He obtained his bachelor's degree from same university in 2020. His research interests include ultra-thick electrodes in batteries and capacitors.

Luyao Zhang is an undergraduate at the School of Automotive Studies of Tongji University. Her current research interests include areas of energy storage systems and fuel cells.

Dr. Jim P. Zheng is a SUNY Empire Innovation Professor at the Department of Electrical Engineering of State University of New York at Buffalo. He was a Sprint Eminent Scholar Chair Professor at the Department of Electrical and Computer Engineering of Florida State University. He is the recipient of National Academy of Inventors Fellow. His research interests include energy storage materials and devices, fuel cells, nano-sensors, photonics, and thin film growth.

Yanyan Lu received her M.S. degree from Xinjiang University in 2020. She is currently a Ph. D. student at the School of Automotive Studies of Tongji University. Her research interests focus on electroochemical capacitors and lithium ion capacitors.

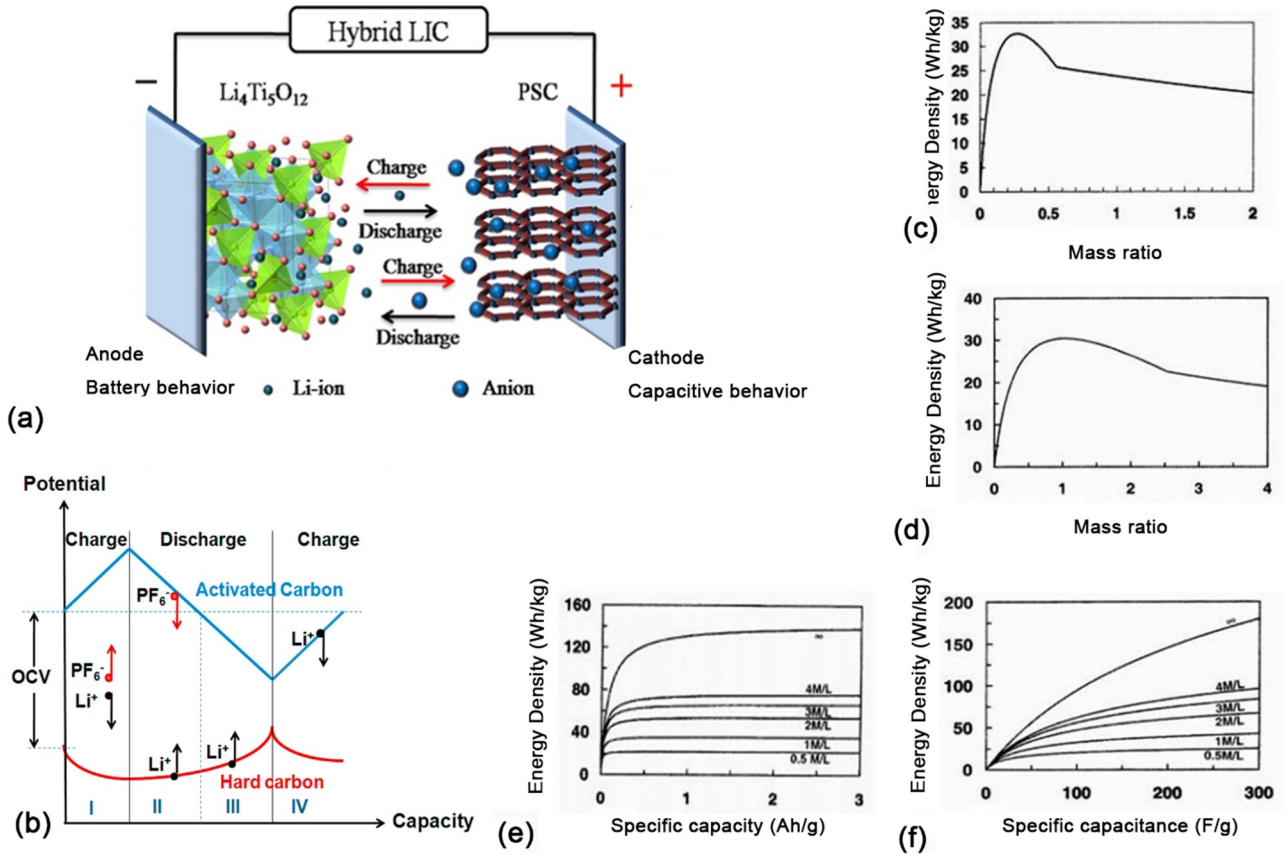

Figure 1. a) Typical device structure and electrode materials of LICs. Reproduced from Ref. [8] with permission. Copyright (2015) Elsevier. b) Diagram of ion transfer in LICs. Reproduced from Ref. [9] with permission. Copyright (2015) Elsevier. And the energy density as a function of electrode mass ratio for c) an AC//$Li_xTi_5O_{12}$ cell and d) an AC//WO_2 cell; the maximum energy density as a function of e) specific capacity of battery electrode and f) specific capacitance of capacitor electrode for different concentrations of electrolyte. Reproduced from Ref. [10] with permission. Copyright (2003) The Electrochemical Society.

unbalance in reaction rate between two electrodes and the power density of LICs depends on the Li-ions insertion/desertion rate in anode. Unlike capacitive electrodes, energy storage achieved by Li-ions inserting into anodes will cause the damage of the anode materials, which limits the cycle life. Therefore, anodes play a critical role in LICs, and attempts to improve anodes have been made. According to the mechanism of energy storage, there are intercalation-type, conversion-type and alloy-type anodes, as shown in Figure 2b. The conversion-type and alloy-type anodes exhibit higher specific capacity but huge volume variation in comparison with the intercalation-type anodes.

The charge-discharge curves of a typical LIC are displayed in Figure 2c. Supposing LIC performs as the linear curve, its power and energy densities can be calculated by the following formulae:

$$E = 0.5\ (V_{max}+V_{min})\ i\ \Delta t \quad (1)$$

$$P = 0.5\ (V_{max}+V_{min})\ i \quad (2)$$

where V_{max} and V_{min} are the maximum and minimum operating cell voltages respectively, i is the current density, Δt is the discharge duration. According to the formulae above, it requires high operating voltage ($V_{max}+V_{min}$), high rate capability (i) and high specific capacity ($i\Delta t$) to achieve high power and energy densities of LICs. Therefore, a promising anode in LICs should have the following merits:

(1) Appropriate voltage plateau, which can obtain higher power and energy densities and avoid risk factors as well.
(2) Excellent rate capability, which aims to match with the high-rate cathode.
(3) High specific capacity, which can offer longer duration.
(4) Long cycling life, which requires to improve anode stability.

2.1. Appropriate Voltage Plateau

As shown in Figure 3a, the maximum energy density has a bearing on the maximum operating voltage. To obtain higher operating voltage, the redox potential of lithiation/delithiation should be lower. However, very low potential will result in Li deposition that is harmful to cell performance. For example, Li deposition on the graphite anodes occurs when potentials below 0.0 V vs Li/Li^+.[16] The charging C-rate has effects on Li deposition,[17] so LICs that work at high rate should pay more attention.

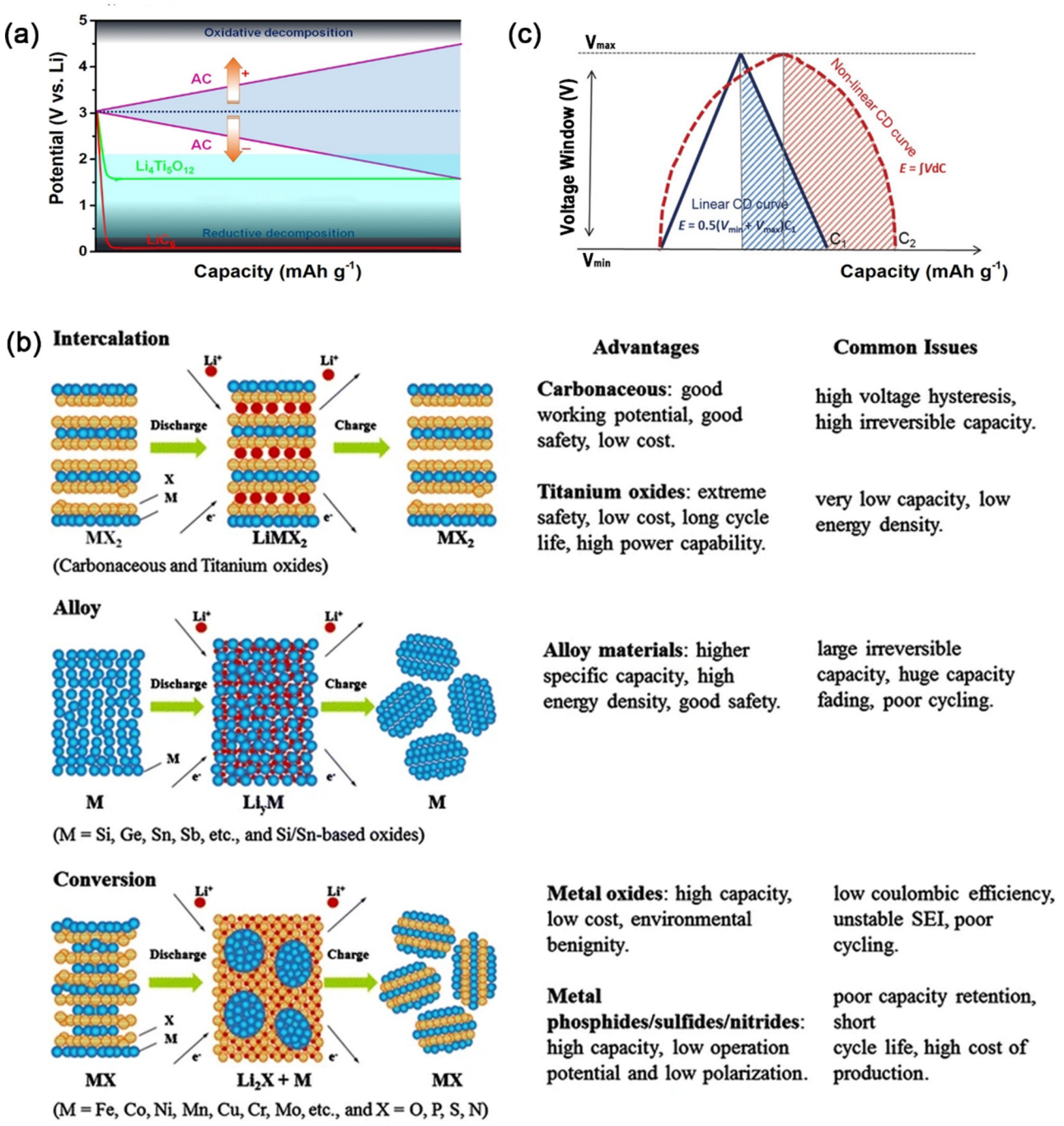

Figure 2. a) Schematic representation of the electrode potentials versus specific capacity for EDLC (pink lines) and Li-insertion electrodes like $Li_4Ti_5O_{12}$ and LiC_6. Reproduced from Ref. [13] with permission. Copyright (2018) American Chemical Society. b) Schematic illustration of three different types of anodes and their advantages and disadvantages. Reproduced from Ref. [14] with permission. Copyright (2018) Springer Nature. c) Schematic of electrochemical profile of a typical LIC. Reproduced from Ref. [15] with permission. Copyright (2017) Wiley-VCH.

Table 1 displays the voltage plateau and specific capacity of different anodes in LICs. It can be seen that materials have higher energy density when they have lower voltage plateau. Cao and coworkers[18] assembled a LIC whose anode is soft carbon and it can deliver energy density of 48 Wh·kg^{-1} and power density of 9 kW·kg^{-1} while it is still stable after 5000 cycles. The LTO materials undergo negligible volume change during the charge-discharge processes, which attracted great attention in the past. However, the high voltage plateau and low specific capacity have restricted its market. In general, converting the valence from Ti^{4+} to Ti^{3+} is the storage mechanism of LTO materials. Recently Liu et al.[23] successfully synthesized Li_2TiSiO_5, which perform lower voltage plateau (~ 0.28 V) and higher specific capacity (>315mAh·g^{-1}) through converting the valence from Ti^{4+} to Ti^{2+}. In 2019, Li and coworkers constructed a LIC with commercial SiO_x/graphite

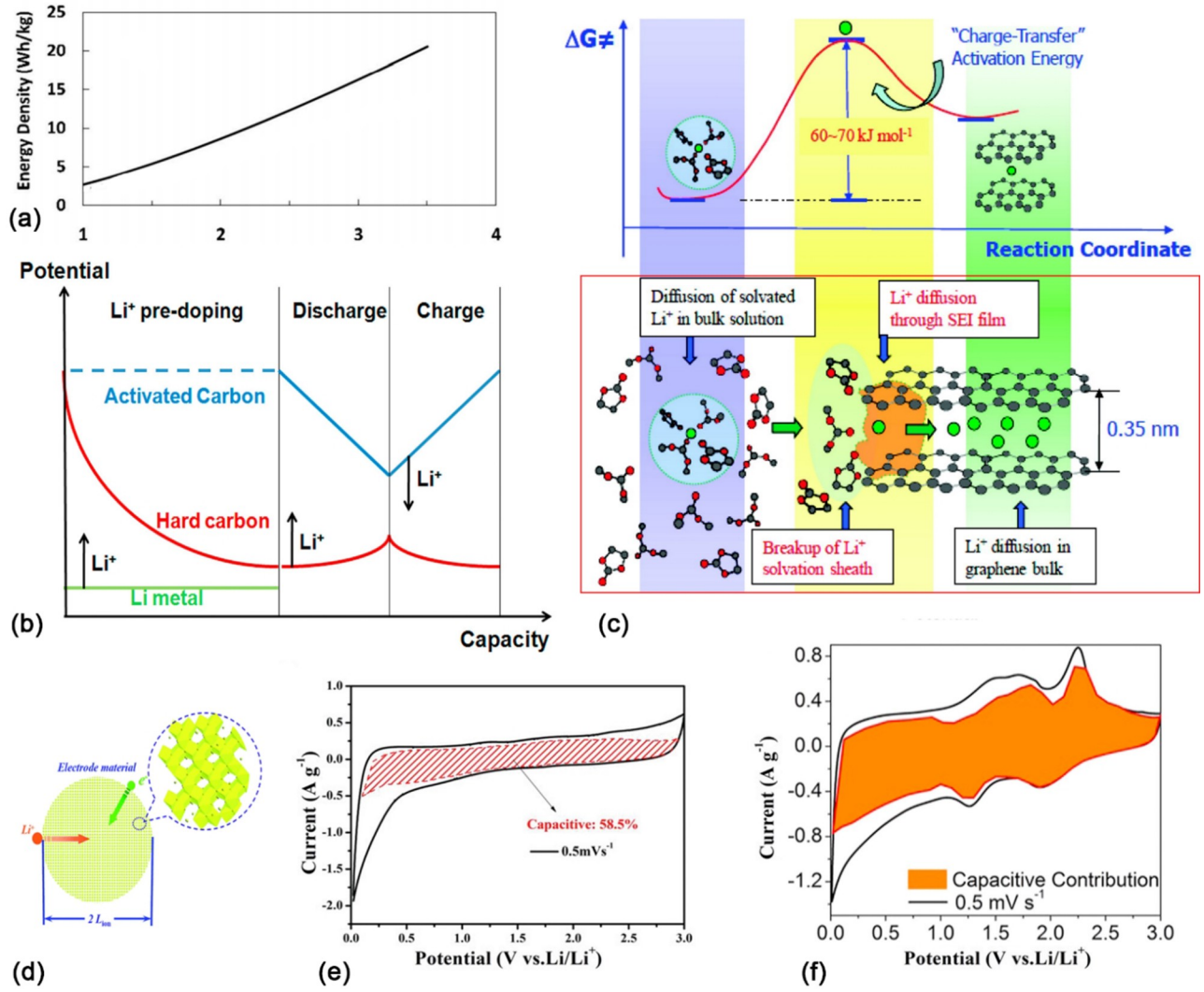

Figure 3. a) The maximum energy density as a function of the maximum operating voltage. Reproduced from Ref. [6] with permission. Copyright (2009) The Electrochemical Society. b) A schematic diagram of the charge transfer during initial charge and discharge cycling. Reproduced from Ref. [9] with permission. Copyright (2015) Elsevier. c) The ions transfer includes the desolvation of Li^+ before it enters interlayers and the subsequent migration of bare Li^+ through interlayers. Reproduced from Ref. [19] with permission. Copyright (2010) American Chemical Society. d) Representative sketch of a charge transfer process that occurs within an intercalation compound particle. Reproduced from Ref. [20] with permission. Copyright (2010) Royal Society of Chemistry. e) The surface capacitive contribution of the carbon nanosheets with nitrogen doping as anode obtained from the CV curve of 0.5 $mV \cdot s^{-1}$. Reproduced from Ref. [21] with permission. Copyright (2019) Wiley-VCH. f) The capacitive contribution of MoS_2-C-rGO electrode at a sweep rate of 0.5 $mV \cdot s^{-1}$. Reproduced from Ref. [22] with permission. Copyright (2017) Elsevier.

Table 1. The electrochemical performances of different anodes.

Electrodes		Voltage Plateau/[V]	Specific Capacity/[$mAh \cdot g^{-1}$]
Intercalation-type	Graphite	0.1	372
	$Li_4Ti_5O_{12}$	1.55	175
Conversion-type	Si	0.4	4200
	Sn	0.6	994
Alloy-type	MnO	0.5	756
	Nb_2O_5	1.5	200

anode and AC cathode, which gave 29.3 $Wh \cdot kg^{-1}$ at 6 $kW \cdot kg^{-1}$ within the voltage range of 1–4 V and obtained high capacitance retention of 95% after 1300 cycles.[24] Wang et al.[25] used modified MnO to assemble a LIC and it performed 90 $Wh \cdot kg^{-1}$ at 1.5 $kW \cdot kg^{-1}$.

Besides that, the pre-doped anodes also can enlarge the operating potentials window to obtain better performance, as depicted in Figure 3b. For example, the open-circuit potential of LIC (graphite *vs.* AC) increases from 0.1 V to 3.1 V after prelithiation.[26] According to the data from Aida and co-

workers,[27] LIC with pre-doped anode gives 1.14 times the energy density and 2.3 times the power density of that without pre-doped anode.

2.2. Excellent Rate Capability

Figure 3d shows a typical charge transfer process on anodes of LIBs. It can be seen that the rate capability of anodes is affected by the diffusion of Li-ions and the transmission of electrons. There have been great efforts on enhancement of the two processes rate recently. Furthermore, generations of SEI may occur at the interface when the electrode contacts with the electrolyte. This film has effects on the diffusion of Li-ions, as depicted in Figure 3c.

Therefore, offering fast and facilitated channels for ions and electrons[28] and changing the storage mechanism[29] are the effective ways to make LICs perform excellent rate capability. The rest of this section discusses these ways in detail.

2.2.1. Change of Storage Mechanism

Although the conversion-type anode has huge volume variation and polarization when storing energy, it attracts much attention in the industry due to its pseudocapacitance. Pseudocapacitance stores energy by utilizing reversible faradic redox reactions on the electrode surface. This faradic charge transfer originates from a very fast sequence of reversible redox, intercalation or electrosorption processes. Study on pseudocapacitance characteristics of anodes is conducive to the improvement of its kinetics. In general, the anode pseudocapacitance can be remarkably promoted by doping heteroatoms. For example, it can be seen from Figure 3e that the pseudocapacitance of mesh-like carbon nanosheets with nitrogen doping contributes to 58.5% of total capacity, while the value is higher than that with no doping (38.3%).[21] Recently, Wu et al.[35] synthesized Ni-doped $MnCo_2O_4$. And attributed to fast Li-ions intercalation pseudocapacitance behavior the Li-ions diffusion coefficient of this materials (1.89×10^{-8} $cm^2\cdot s^{-1}$) is higher than $MnCo_2O_4$ (7.54×10^{-9} $cm^2\cdot s^{-1}$).

Recently, some transition metal oxides present pseudocapacitive properties in non-aqueous electrolyte, which makes them a promising anode for LICs. MoS_2 is a typical two dimensional material and its layers connect by weak van der Waals force with an interlayer spacing of 0.62 nm which the large gaps facilitate the fast Li-ions insertion.[36] Beyond that, it has been reported that during the Li-ions intercalation/deintercalation process the MoS_2 anode performs pseudocapacitive properties. However, the theoretical specific capacity of this process is only 167 $mAh\cdot g^{-1}$ and its redox potential is high (>1 V, *vs* Li/Li^+), resulting in a limited energy density of the corresponding LIC.[37] Wang and coworkers have made efforts on combination of carbon and reduced graphene oxide (rGO) and MoS_2, and this new material performs excellent properties with high specific capacity of 375 $mAh\cdot g^{-1}$ at 10 $A\cdot g^{-1}$ and the pseudocapacitive contribution reaches 79.3%, as depicted in Figure 3f.[22]

2.2.2. Optimization on Anodes Structure

The diffusion process of Li-ions is related to its diffusion length and its diffusion coefficient in electrode.[20] The diffusion duration can be calculated as follow:

$$\tau = L_{ion}^{\ 2}/D_{Li} \quad (3)$$

where L_{ion} is lithium diffusion length, and D_{Li} is Li-ions diffusion coefficient. Moreover, L_{ion} is related to the thickness of electrode materials and D_{Li} depends on inherent materials characteristic. Therefore, effective strategies to improve rate performance of anodes are to diminish particle size for shortening the length or to heighten the coefficient.

Cai and coworkers synthesized hierarchical porous TiO_2 microspheres by a solvothermal method.[30] This material was composed of microspheres that were built by many nanosheets and the structure enables the electrolyte to fully infiltrate the electrode for shortening the diffusion length of Li-ions. Subsequently, they assembled a LIC by using the TiO_2 microspheres and commercial AC. The LIC showed prominent electrochemical properties, which obtained the energy density of 31.5 $Wh\cdot kg^{-1}$ at the power density of 9.45 $kW\cdot kg^{-1}$ and its capacity retention and columbic efficiency reaches 98% and 95% after 1000 cycles respectively, as shown in Figure 4a. And a team fabricates porous lithium titanate anode that its nanostructured particle size and penetrating lithium ion transmission channels could improve lithium ion diffusion coefficient.[31] It can be proved in Figure 4b, A_w is Warburg coefficient and D_{Li} is inversely proportional to A_w.

For the intercalation-type materials, widening the interlayer spacing can facilitate the diffusion of Li-ions. Researchers have made distinct attempts to make it a reality, such as adding functional groups or doping inorganic elements. For example, Jin et al.[32] enlarged the interlayer spacing of graphene (0.34 ~ 0.77 nm) by carboxyl groups modification. And its corresponding LIC performed better rate capability and cycling stability than HC, as shown in Figure 4c–d. Moreover, Xia and coworkers also enlarged the interlayer spacing of graphite from 0.38 to 0.49 nm by doping B and N.[38] Subsequently, they have constructed a LIC with BNC as both anode and cathode and it exhibits improved electrochemical performance, which can deliver energy density of 104 $Wh\cdot kg^{-1}$ at the power density of 22.5 $kW\cdot kg^{-1}$ with the capacity retention of 81% after 5000 cycles.

Due to the abundant active site on surface to offer shorter diffusion length and an open layered structure to facilitate the diffusion of Li-ions, the two-dimensional materials have attracted enormous attention to its application as anode in LICs in recent years. In 2011, Prof. Gogotsi and Prof. Barsoum synthesized a new two-dimensional material that is two dimensional transition metal oxides, nitrides and carbonitrides (MXenes). $Ti_3C_2T_x$ is a typical MXenes, and Tang et al. used

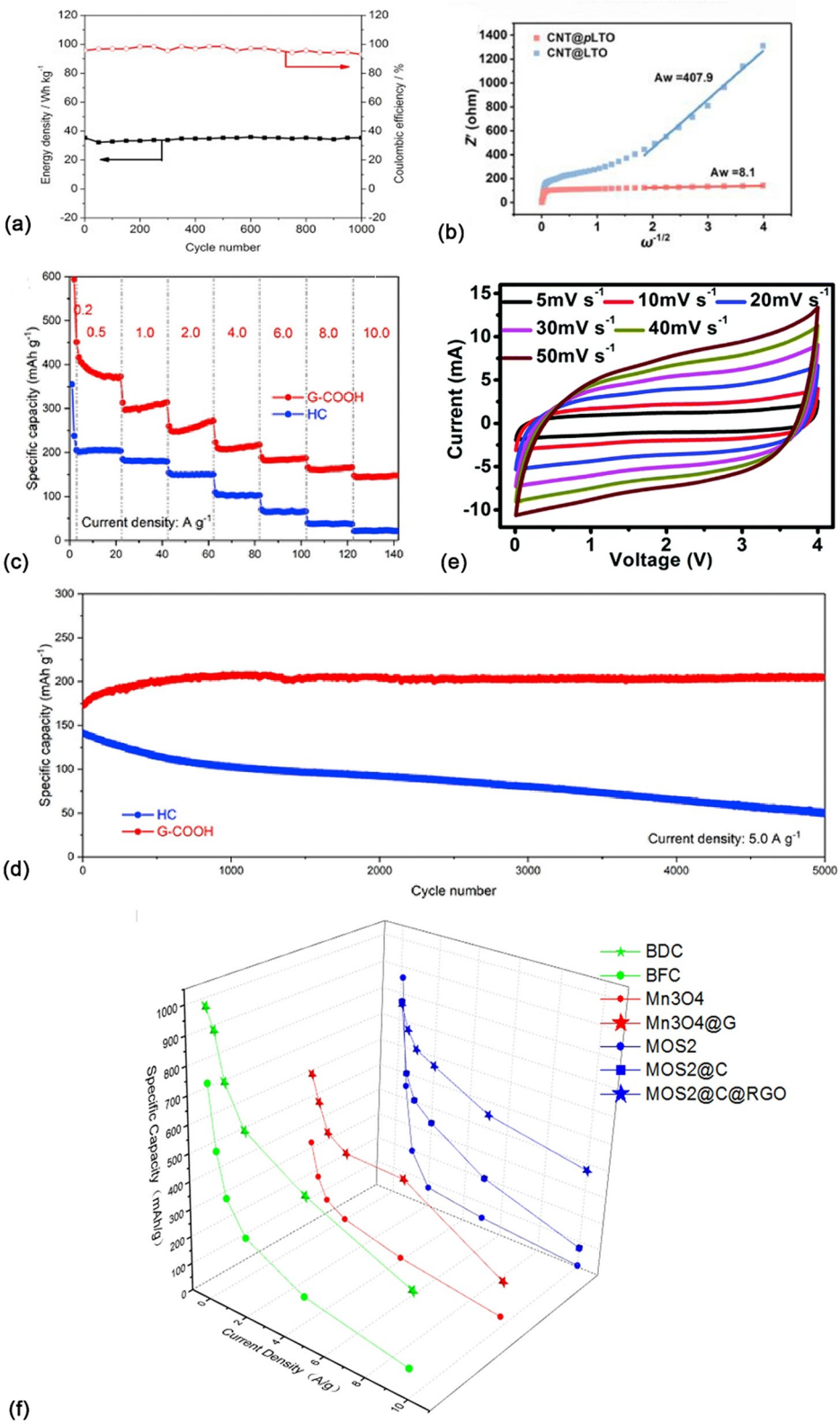

Figure 4. a) Cycling stability in energy density and coulombic efficiency versus cycle number for AC//TiO_2 LIC. Reproduced from Ref. [30] with permission. Copyright (2014) Elsevier. b) Diffusion coefficient calculated based on EIS. Reproduced from Ref. [31] with permission. Copyright (2020) Science Press and Dalian Institute of Chemical Physics, Chinese Academy of Sciences. c) The multi-rate performance from 0.2 to 10 $mA \cdot g^{-1}$ and d) the long cycling performance at 5.0 $A \cdot g^{-1}$ of G-COOH and HC. Reproduced from Ref. [32] with permission. Copyright (2019) Elsevier. e) The CV curves of the $Ti_3C_2T_x$@ Fe_2CO_3//NS-DPC LIC device. Reproduced from Ref. [33] with permission. Copyright (2018) Royal Society of Chemistry. f) The rate performance of some materials after modification, and these data can be obtained from Refs. [22, 34].

Table 2. Components of SEI under certain conditions.

Component	Equation	Notes
$(CH_2OCO_2Li)_2$	$EC + 2e^- + 2Li^+ \rightarrow (CH_2OCO_2Li)_2\downarrow + C_2H_4(g)\uparrow$	It is a reduction of EC.[43]
$ROCO_2Li$	$PC + 2e^- + 2Li^+ \rightarrow ROCO_2Li + Li_2CO_3\downarrow + C_3H_6(g)\ \uparrow$	It is found in the electrolyte containing PC.[43]
Li_2CO_3	$(CH_2OCO_2Li)_2 + H_2O \rightarrow Li_2CO_3\downarrow + (CH_2OH)_3\downarrow + CO_2(g)\ \uparrow(1)$ $PC + 2e^- + 2Li^+ \rightarrow ROCO_2Li + Li_2CO_3\downarrow + C_3H_6(g)\ \uparrow(2)$	There is EC (1) or PC(2) in the electrolyte.[43]
ROLi	$DMC + e^- + Li^+ \rightarrow CH_3OCCOOLi\downarrow + 0.5\ C_2H_6$	It appears as a reduction product of DEC or EMC.[44]
LiF	$LiPF_6 + e^- + Li^+ \rightarrow LiF + Li_xPF_y$	There are salt fluorides, such as $LiPF_6$ and $LiAsF_6$.[45]
Li_2O	$Li_2CO_3 \rightarrow Li_2O + CO_2(g)\ \uparrow$	It may be a degradation product of Li_2CO_3.
LiOH	trace $H_2O + e^- + Li^+ \rightarrow LiOH + 1/2H_2$	It mainly due to water contamination[45]

Fe_2CO_3 as pillars between $Ti_3C_2T_x$ layers to offer more active sites and to enlarge the interlayer spacing to 1 nm.[33] And the shape of cyclic voltammetry curves of a LIC with $Ti_3C_2T_x$@Fe_2CO_3 anode is near rectangular, which indicates the outstanding rate performance and the existence of pseudocapacitance, as depicted in Figure 4e. And this cell can deliver energy density of 96.5 $Wh\cdot kg^{-1}$ at power density of 20 $kW\cdot kg^{-1}$. It is not a unique instance. Li et al. expand the Ti_3C_2 interlayer space by the intercalation of TiO2 nanoparticles and rGO which shortens the ion diffusion path and promotes the electrolyte transport.[39]

Since the charge transfer process is the diffusion of Li-ions as well as the transmission of electrons, to improve conductivity is essential. Except for enlarging the interlayer spacing, the heteroatom doping method can also enhance electrochemical conductivity.[40] And compositing anodes with the fast conductive grid is an efficient way to increase conductivity as well, and Gao et al.[41] have proved that. Recently, Yang and coworkers used polydopamine/graphene composite anode and porous graphene cathode to assemble asymmetric capacitor. The study indicates that the 2D nature of polydopamine/graphene is convenient for ions transport and graphene facilitates electrons transfer. And this cell can deliver energy density of 78.9 $Wh\cdot kg^{-1}$ at power density of 21.0 $kW\cdot kg^{-1}$.[42]

To summarize, Figure 4f shows the improved rate capacity of some materials after modification. Therefore, the optimal structure with high energy and power densities is shown to be a structure that can shorten the diffusion length and heighten the diffusion coefficient. One of that is an ordered mesoporous structure, its high porosity can facilitate the diffusion of Li-ions, and its ordered structure can provide fast and versatile pathways for both ions and electrons.[20]

2.2.3. Enhancement of SEI Electrochemical Performance

When there is SEI between the electrode and electrolyte, its priorities are the transmission of Li-ions and the insulation of electrons. Table 2 gives some species of SEI under certain conditions. Due to the complex components of SEI, there are multi pathways for the transmission of Li-ions which are generally via grain boundaries (GBs) and crystal phases. These main crystal phases are LiF, Li_2O, Li_2CO_3, Li_3N. It can be known from Table 3 that these components have an electronic transfer barrier of $LiF > Li_2CO_3 > Li_2O > Li_3N$ and an ionic migration barrier of $LiF > Li_2CO_3 > Li_2O > Li_3N$, which means that Li_3N is a better channel for Li-ions but also electrons.[46] Furthermore, there are multi pathways for fast Li-ions conduction in GBs. As shown in Figure 5a–b, from the research on GBs among the three main inorganic components (LiF, Li_2O, Li_2CO_3) in SEI, the performance is listed in Table 4 and the diffusion of Li-ions in GBs between LiF and Li_2O is more convenient.[47] It is reported that the diffusion coefficient of Li-ions in LiF crystal is 10^{-26}~10^{-20} $m^2\cdot s^{-1}$ and the value in Li_2O is 10^{-16} $m^2\cdot s^{-1}$.[48] Compared with the data in Table 4, it indicates that the diffusion of Li-ions in GBs is faster than that in crystal phase.

Table 3. Ionic and electronic properties of species in a SEI film.[46]

Species	Energy barrier of Li migration [eV]	Band gap [eV]
Li_2O	0.15	4.7
Li_3N	0.007-0.038	1.1
LiF	0.73	8.9
Li_2CO_3	0.23-0.49	5.0

From Table 3, LiF has low conductivity and is considered as an excellent passivation component in SEI. Recently, researchers attempted to enhance the low diffusion coefficient of Li-ions in LiF crystal by the aid of GBs. For example, Zhang and coworkers[49] constructed SEI with the coexistence of LiF and Li_2CO_3, as shown in Figure 5c. It has demonstrated that LiF plays an essential role in enhancement of cycling stability and the synergistic effects of LiF and Li_2CO_3 facilitate the transmission of Li-ions.[49]

Therefore, the ideal components of SEI might be the coexistence of LiF and Li_2CO_3. The GBs create more pathways for lithium ions and the defects near the interface make Li_2CO_3 more insulated by consuming the electrons nearby, and LiF

Table 4. Summary of ALL activation energies and diffusion coefficients for Li diffusion in the respective GB.[47]

GB	Activation energy [eV]	Diffusion coefficient [$m^2\cdot s^{-1}$]
LiF/LiF (Σ5 GB)	0.68	4.6×10^{-16}
LiF/LiF (Σ3 GB)	1.03	3.16×10^{-23}
Li_2O/Li_2O (Σ15 GB)	0.78	7.38×10^{-16}
LiF/Li_2O	0.45	3.87×10^{-14}

itself is a good insulator. It is a guidance to pay attention to the synergism of species of SEI.

2.3. Long Cycling Life

The cycling stability is the main challenge for the commercial applications of LICs. Due to the stress variation during the charge-discharge processes, the active particles in anodes would crack. It is regarded as the main mechanism of anode degradation, as depicted in Figure 6a. Firstly, the cracks can weight against electric conductivity and even some active particles would fall off from the collector. Secondly, the cracks make the electrode get in touch with the electrolyte and the new SEI is generated, which means the storage species irreversibly consume and the impedance increases. Finally, the consumption of electrolyte would affect the wettability of the electrode, which prolongs the diffusion length of Li-ions.

2.3.1. Improvement of SEI Stability

Distinct models have been developed to describe the spatial distribution of SEI. At present, the "mosaic" model and the multilayer model attract the most attention (Figure 6b). Both structures have been observed in experiments.[55] In the former model, the organic and inorganic reduction products of electrolytes are randomly dispersed. The distribution of organic and inorganic in the latter model is more regular. Generally, the low-oxidation inorganic substances distributing in the inner layer makes it dense, whereas the outer layer which is made up of high-oxidation organic order is porous. The reason for this distribution is related to decomposition sequence of species in electrolyte and subsequent evolution.

Despite the distinct morphology of these two models, Cheng et al. put forward views that the two models are not contradictory and propose a new comprehensive model that SEI is composed of multilayers and the species in each layer distribute as the mosaic model.[46] However, a team studied on the two SEI models on Li anode and found that Li stripping in ordered multilayer structure is more well-distributed, as depicted in Figure 6c.[52] And it is not clear whether this difference will have the same effects on other anodes.

Given this, this paper suggests that it should be promoted to generate the multilayer SEI structure. For example, it is reported that a new lithium electrolyte salts (LiBOB) can break down into a film on the electrode surface and deliver a better cycling capacity at high temperature.[29a] Yu and coworkers coated an ultrathin Al_2O_3 film on ZnO-graphene anode by using atomic layer deposition craft and the anode performed excellent cycling stability.[56]

Beyond that, the prelithiation craft also has effects on SEI stability. Lee et al.[53] have investigated the effects on SEI in SiO_x anodes about the processing time of prelithiation and discovered that SEI shows the best morphology after the processing time of 12 h, as depicted in Figure 6d. And the anode exhibits outstanding capacity retention of 88.6% over 500 cycles with a high coulombic efficiency of 99%. It reminds us that to pay attention to the formed conditions of SEI is essential.

2.3.2. Appropriate Working Potential

It has been demonstrated that anodes deliver distinct performances under different working potentials. Take HC for example, its electrochemical process can be divided into four regions, as shown in Figure 6e. In region I, the HC anode stores energy by adsorption-desorption mechanism at its defects and the morphology of HC remains unchanged. In region II, the anode stores energy by intercalation-deintercalation mechanism, but its kinetics is slow due to the small interlayer spacing. In region IV, the anode also exhibits slow kinetics behavior and even poor stability. The reason why is that there are too many Li-ions between layers to accommodate new ions and the large strain of materials leads to poor cycling stability due to the many intercalated ions. Besides that, too low potential may bring out Li deposition. On the contrary, there are larger interlayer spacing, abundant active sites and low material strain in region III.[54] Therefore, to choose this working potential

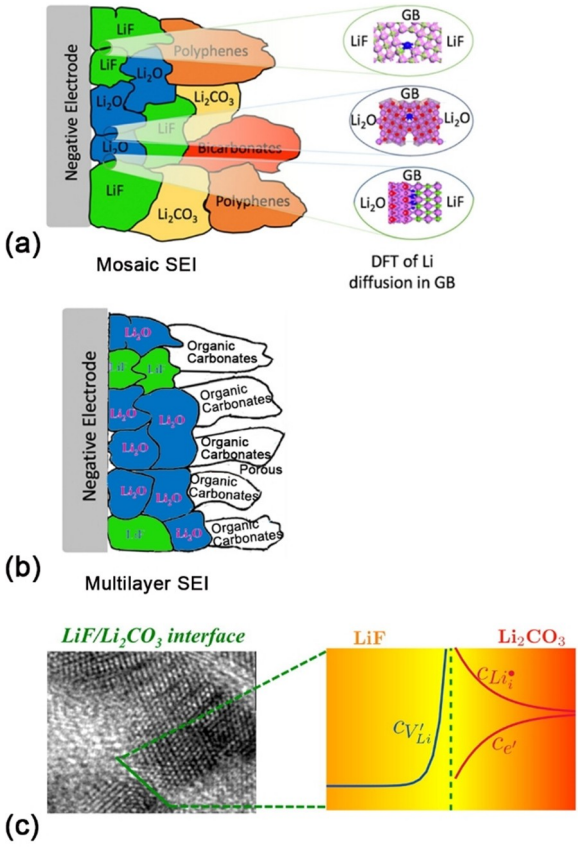

Figure 5. a) The schematic diagram of grain boundary. Reproduced from Ref. [47] with permission. Copyright (2019) American Chemical Society. b) The diagram shows the same grain boundary as the above diagram, and it is drawn on the basis of the study of Wang and co-workers from Ref. [50]. c) The transmission of Li-ion in GB. Reproduced from Ref. [49] with permission. Copyright (2016) American Chemical Society.

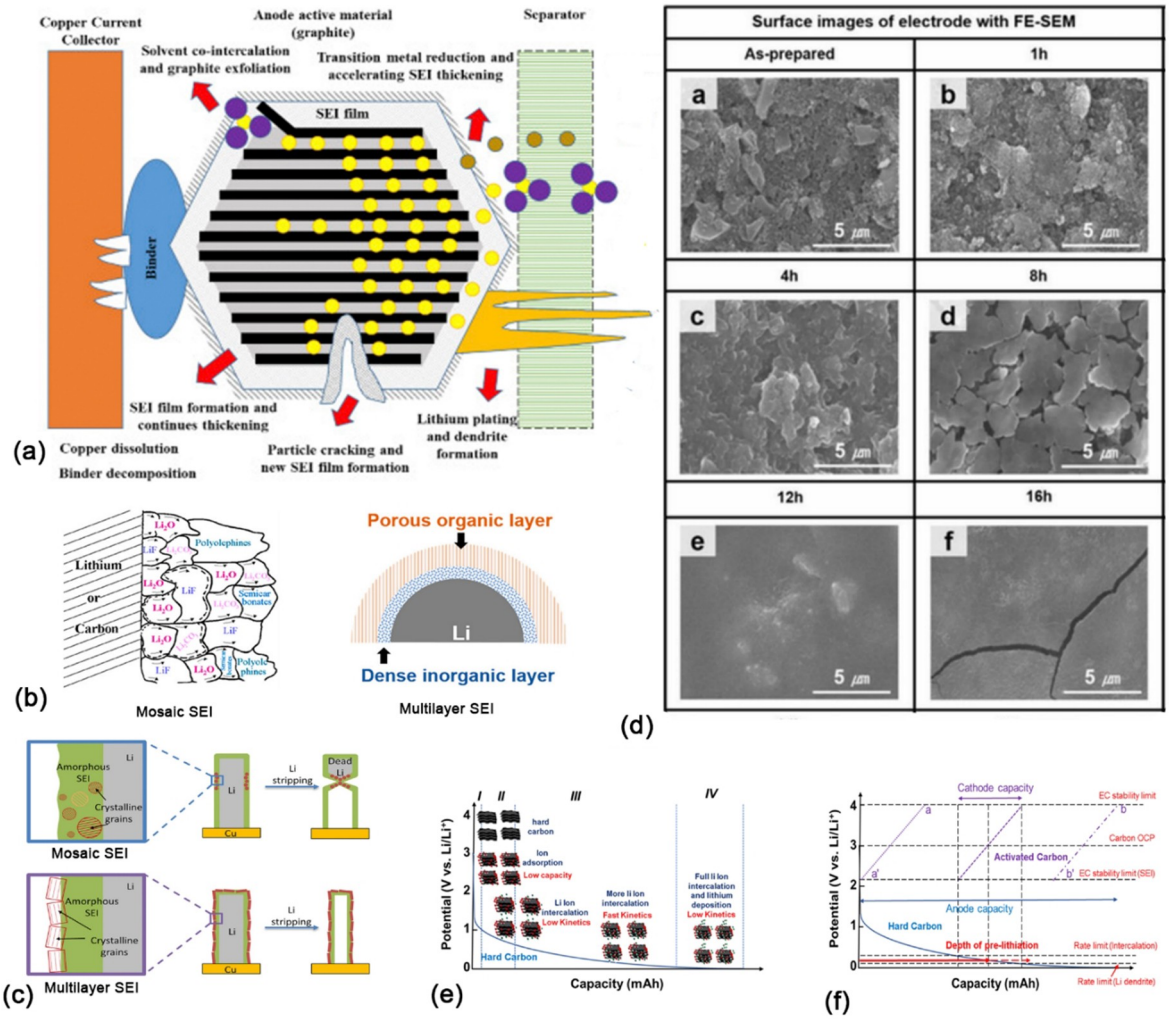

Figure 6. a) Schematic diagram of the anode degradation. Reproduced from Ref. [51] with permission. Copyright (2019) Elsevier. b) The schematic diagram of the "mosaic" model and the multilayer model. Reproduced from Ref. [46] with permission. Copyright (2018) American Chemical Society. c) Li metal deposition and stripping morphology with mosaic and multilayer SEI structure. Reproduced from Ref. [52] with permission. Copyright (2018) Elsevier. d) SEM micrographs of electrode surface after different processing time. Reproduced from Ref. [53] with permission. Copyright (2019) The Electrochemical Society. e) The reaction mechanism scheme image of HC anode; f) The scheme graph of a practical and universal approach for electrode matching for LICs. Reproduced from Ref. [54] with permission. Copyright (2019) Elsevier.

range can deliver an outstanding rate and cycling performances for LICs.

Recently, Jin and coworkers[54] have proposed a new approach to choose the appropriate working potential to match the kinetics of two electrodes. This approach can be simply considered as a three-step process, as above in Figure 6f. Firstly, EIS and other technologies can be used to choose the best working potential range and the corresponding capacity of anodes. Secondly, to regulate the anode potential can use the prelithiation craft by adjusting the loadings. Finally, the potential of the cell is determined by the operating potentials of two electrodes.

Moreover, researchers have made great efforts to search appropriate anodes to deliver ideal rate and cycling performance. From the above, it gives the industry a new insight that the promising anode can perform an excellent electrochemical property at only a certain potential range. Considering this, some old materials can be brought a new life in LICs.

3. Conclusions

LICs are considered as high power density and high energy density cells and they have broad prospects in rail traffic and new energy vehicles. The introduction of battery-type anodes is aimed to improve the cell energy density. Nevertheless, battery-type anodes affect conversely the cell power density and cycling life due to its storage mechanism. Therefore, the electrochemical performance of LICs is highly related to anodes and many attempts have been made to improve it.

To sum up, the following rules can guide the orientation to search for ideal anodes:

(1) The ideal anodes should work at a low plateau voltage but not too low, such as 0.3–0.7 V vs Li/Li+. The high voltage would lessen energy density and the low voltage would deteriorate cycling performance. And the structure of anodes can provide shorter diffusion length and higher diffusion coefficient of Li-ions, such as the ordered mesoporous structure.
(2) The fast kinetics of anodes should be considered as the main research direction, not the high capacity. And pseudocapacitive behavior can be regarded as the transition state of battery-type energy storage and capacitor-type energy storage, which has good effects on cycling and rate performances of LICs. It is essential to pay attention to pseudocapacitive behavior.
(3) The ideal structure of SEI should be the multilayer structure and the inner layer might be the coexistence of LiF and Li_2CO_3, whose synergistic effects achieve better ionic conductivity and electronic insulation. And study on the synergism between SEI components could bring fresh insights unlike single ingredients.
(4) The prelithiation and the optimal working potential range play an important role in the electrochemical properties of anodes. From the commercial perspective, to optimize the operation condition is the most economical ways of improving the LICs performance, and it is of great significance for productivity, costs and safety.

Acknowledgements

The work is supported by National Science Foundation of China, Grant No. 51777140, and the Fundamental Research Funds for the Central Universities at Tongji University, Grant No. 17002150019.

Conflicts of interest

There are no conflicts to declare.

Keywords: lithium-ion capacitors · anodes · solid–electrolyte interface · operation condition

[1] F. B. Glenn, G. Amatucci, A. D. Pasquier, T. Zheng, *The Electrochem. Soc.* **2001**, *148*, A930–A939.
[2] X. Han, P. Han, J. Yao, S. Zhang, X. Cao, J. Xiong, J. Zhang, G. Cui, *Electrochim. Acta* **2016**, *196*, 603–610.
[3] G. Wang, Z. Y. Liu, J. N. Wu, Q. Lu, *Mater. Lett.* **2012**, *71*, 120–122.
[4] S. H. Lee, G. Yoo, J. Cho, S. Ryu, Y. S. Kim, J. Yoo, *J. Alloys Compd.* **2020**, *829*.
[5] Ultracapacitor requirements from USABC, http://www.uscar.org/guest/article_view.php?articles_id=85.
[6] J. P. Zheng, *J. Electrochem. Soc.* **2009**, *156*, A500-A505.
[7] C. Yan, H. Yuan, H. S. Park, J. Q. Huang, *J. Energy Chem.* **2020**, *47*, 217–220.
[8] S. Dong, X. Wang, L. Shen, H. Li, J. Wang, P. Nie, J. Wang, X. Zhang *J. Electroanal. Chem.* **2015**, *757*, 1–7.
[9] W. J. Cao, M. Greenleaf, Y. X. Li, D. Adams, M. Hagen, T. Doung, J. P. Zheng, *J. Power Sources* **2015**, *280*, 600–605.
[10] J. P. Zheng, *J. Electrochem. Soc.* **2003**, *150*, A484-A492.
[11] S. K. Heiskanen, J. Kim, B. L. Lucht, *Joule* **2019**, *3*, 2322–2333.
[12] A. J. Louli, L. D. Ellis, J. R. Dahn, *Joule* **2019**, *3*, 745–761.
[13] V. Aravindan, Y. S. Lee, *J. Phys. Chem. Lett.* **2018**, *9*, 3946–3958.
[14] J. Lu, Z. Chen, F. Pan, Y. Cui, K. Amine, *Electrochem. Energy Rev.* **2018**, *1*, 35–53.
[15] H. Wang, C. Zhu, D. Chao, Q. Yan, H. J. Fan, *Adv. Mater.* **2017**, *29*.
[16] N. Legrand, B. Knosp, P. Desprez, F. Lapicque, S. Raël, *J. Power Sources* **2014**, *245*, 208–216.
[17] T. Waldmann, B. I. Hogg, M. W. Mehrens, *J. Power Sources* **2018**, *384*, 107–124.
[18] W. Cao, J. Zheng, D. Adams, T. Doung, J. P. Zheng, *J. Electrochem. Soc.* **2014**, *161*, A2087-A2092.
[19] K. Xu, A. von Cresce, U. Lee, *Langmuir* **2010**, *26*, 11538–11543.
[20] Y. Wang, H. Li, P. He, E. Hosono, H. Zhou, *Nanoscale* **2010**, *2*, 1294–1305.
[21] Z. Li, L. Cao, W. Chen, Z. Huang, H. Liu, *Small* **2019**, *15*, e1805173.
[22] R. Wang, S. Wang, D. Jin, Y. Zhang, Y. Cai, J. Ma, L. Zhang, *Energy Storage Mater.* **2017**, *9*, 195–205.
[23] J. Liu, W. K. Pang, T. Zhou, L. Chen, Y. Wang, V. K. Peterson, Z. Yang, Z. Guo, Y. Xia, *Energy Environ. Sci.* **2017**, *10*, 1456–1464.
[24] C. Li, X. Zhang, K. Wang, X. Sun, Y. Ma, *J. Power Sources* **2019**, *414*, 293–301.
[25] H. Wang, Z. Xu, Z. Li, K. Cui, J. Ding, A. Kohandehghan, X. Tan, B. Zahiri, B. C. Olsen, C. M. Holt, D. Mitlin, *Nano Lett.* **2014**, *14*, 1987–1994.
[26] S. R. Sivakkumar, A. G. Pandolfo, *Electrochim. Acta* **2012**, *65*, 280–287.
[27] T. Aida, K. Yamada, M. Morita, *Electrochem. Solid-State Lett.* **2006**, *9*, A534-A536.
[28] a) P. Chen, W. Zhou, Z. Xiao, S. Li, H. Chen, Y. Wang, Z. Wang, W. Xi, X. Xia, S. Xie, *Energy Storage Mater.* **2020**, *33*, 298–308; b) H. Jiang, S. Wang, B. Zhang, Y. Shao, Y. Wu, H. Zhao, Y. Lei, X. Hao, *Chem. Eng. J.* **2020**, *396*.
[29] a) Z. Chen, Y. Qin, Y. Ren, W. Lu, C. Orendorff, E. P. Roth, K. Amine, *Energy Environ. Sci.* **2011**, *4*; b) J. Boltersdorf, S. A. Delp, J. Yan, B. Cao, J. P. Zheng, T. R. Jow, J. A. Read, *J. Power Sources* **2018**, *373*, 20–30; c) K. Xu, *Chem. Rev.* **2014**, *114*, 11503–11618.
[30] Y. Cai, B. Zhao, J. Wang, Z. Shao, *J. Power Sources* **2014**, *253*, 80–89.
[31] Y. Liu, W. Wang, J. Chen, X. Li, Q. Cheng, G. Wang, *J. Energy Chem.* **2020**, *50*, 344–350.
[32] L. Jin, X. Guo, R. Gong, J. Zheng, Z. Xiang, C. Zhang, J. P. Zheng, *Energy Storage Mater.* **2019**, *23*, 409–417.
[33] X. Tang, H. Liu, X. Guo, S. Wang, W. Wu, A. K. Mondal, C. Wang, G. Wang, *Mater. Chem. Front.* **2018**, *2*, 1811–1821.
[34] a) F. Sun, H. B. Wu, X. Liu, F. Liu, R. Han, Z. Qu, X. Pi, L. Wang, J. Gao, Y. Lu, *Mater. Today* **2018**, *9*, 428–439; b) C. Liu, Q. Ren, S. Zhang, B. Yin, L. Que, L. Zhao, X. Sui, F. Yu, X. Li, D. Gu, Z. Wang, *Chem. Eng. J.* **2019**, *370*, 1485–1492.
[35] L. Wu, J. Lang, S. Wang, P. Zhang, X. Yan, *Electrochim. Acta* **2016**, *203*, 128–135.
[36] C. Lee, H. Yan, L. E. Brus, T. F. Heinz, J. Hone, S. Ryu, *J. Am. Chem. Soc.* **2010**, *4*, 2695–2700.
[37] J. B. Cook, H. Kim, Y. Yan, J. Ko, S. Robbennolt, B. Dunn, S. H. Tolbert, *Adv. Energy Mater.* **2016**, *6*.
[38] Q. Xia, H. Yang, M. Wang, M. Yang, Q. Guo, L. Wan, H. Xia, Y. Yu, *Adv. Energy Mater.* **2017**, *7*.
[39] Z. Li, G. Chen, J. Deng, D. Li, T. Yan, Z. An, L. Shi, D. Zhang, *ACS Sustainable Chem. Eng.* **2019**, *7*, 15394–15403.
[40] J. P. Paraknowitsch, A. Thomas, *Energy Environ. Sci.* **2013**, *6*.
[41] C. Gao, H. Zhao, P. Lv, C. Wang, J. Wang, T. Zhang, Q. Xia, *J. Electrochem. Soc.* **2014**, *161*, A2216-A2221.
[42] Y. Yang, Q. Lin, B. Ding, J. Wang, V. Malgras, J. Jiang, Z. I. Li, S. Chen, H. Dou, S. M. Alshehri, T. Ahamad, J. Na, X. Zhang, Y. Yamauchi, *Carbon* **2020**, 627–633.
[43] V. A. Agubra, J. W. Fergus, *J. Power Sources* **2014**, *268*, 153–162.
[44] T. Liu, L. Lin, X. Bi, L. Tian, K. Yang, J. Liu, M. Li, Z. Chen, J. Lu, K. Amine, K. Xu, F. Pan, *Nat. Nanotechnol.* **2019**, *14*, 50–56.
[45] P. Lu, C. Li, E. W. Schneider, S. J. Harris, *J. Phys. Chem. C* **2014**, *118*, 896–903.
[46] X. Cheng, C. Yan, X. Zhang, H. Liu, Q. Zhang, *ACS Energy Lett.* **2018**, *3*, 1564–1570.
[47] A. Ramasubramanian, V. Yurkiv, T. Foroozan, M. Ragone, R. Shahbazian-Yassar, F. Mashayek, *J. Phys. Chem. C* **2019**, *123*, 10237–10245.
[48] a) H. Yildirim, A. Kinaci, M. K. Chan, J. P. Greeley, *ACS Appl. Mater. Interfaces* **2015**, *7*, 18985–18996; b) K. Tasaki, A. Goldberg, J. Lian, M.

Walker, A. Timmons, S. J. Harris, *The Electrochem. Soc.* **2009**, *156*, A1019–A1027.
[49] Q. Zhang, J. Pan, P. Lu, Z. Liu, M. W. Verbrugge, B. W. Sheldon, Y. T. Cheng, Y. Qi, X. Xiao, *Nano Lett.* **2016**, *16*, 2011–2016.
[50] Y. Zhou, M. Su, X. Yu, Y. Zhang, J. Wang, X. Ren, R. Cao, W. Xu, D. R. Baer, Y. Du, O. Borodin, Y. Wang, X. Wang, K. Xu, Z. Xu, C. Wang, Z. Zhu, *Nat. Nanotechnol.* **2020**, *15*, 224–230.
[51] X. Han, L. Lu, Y. Zheng, X. Feng, Z. Li, J. Li, M. Ouyang, *eTransportation* **2019**, *1*.
[52] Y. Li, W. Huang, Y. Li, A. Pei, D. T. Boyle, Y. Cui, *Joule* **2018**, *2*, 2167–2177.
[53] D. I. Lee, H. W. Yang, W. S. Kang, J. Kim, S. J. Kim, *J. Electrochem. Soc.* **2019**, *166*, A787–A792.
[54] L. Jin, X. Guo, C. Shen, N. Qin, J. Zheng, Q. Wu, C. Zhang, J. P. Zheng, *J. Power Sources* **2019**, *441*.
[55] Y. Li, Y. Li, A. Pei, K. Yan, Y. Sun, C. Wu, L. Joubert, R. Chin, A. L. Koh, Y. Yu, J. Perrino, S. Chu, B. Butz, Y. Cui, *Science* **2017**, *358*, 506–510.
[56] M. Yu, A. Wang, Y. Wang, C. Li, G. Shi, *Nanoscale* **2014**, *6*, 11419–11424.

Manuscript received: November 27, 2020
Revised manuscript received: December 28, 2020
Accepted manuscript online: January 3, 2021
Version of record online: February 17, 2021